Mechanism and Machine Theory 113 (2017) 109–125

Contents lists available at ScienceDirect

Mechanism and Machine Theory

journal homepage: www.elsevier.com/locate/mechmachtheory

Research paper

Gear shift control of a dual-clutch transmission using optimal control allocation

Sooyoung Kim[a], Jiwon Oh[b], Seibum Choi[a,*]

[a] Department of Mechanical Engineering, Korea Advanced Institute of Science and Technology, 291 Daehak-ro Yuseong-gu, Daejeon 307-701, Republic of Korea
[b] Eco-vehicle Control System Development Team, Hyundai Motor Company, 150 Hyundaeyeonguso-ro, Hwaseong-si, Gyeonggi-do, Republic of Korea

ARTICLE INFO

Article history:
Received 4 October 2016
Revised 22 January 2017
Accepted 28 February 2017
Available online 18 March 2017

Keywords:
Dual-clutch transmission
Gear shift control
Control allocation
Clutch-to-clutch shift control

ABSTRACT

This study develops control strategies for the gear shift of dual-clutch transmissions (DCTs) using optimal control allocation. DCT powertrains require sophisticated control of two clutch actuators and the engine throttle to achieve good shift performances, i.e. smooth and fast gear shifts. In this paper, a new approach to the control strategies is implemented through interpreting the DCT powertrain as an over-actuated system that possesses actuator redundancy. The developed control structure is divided into two stages: the upper level control that governs the procedure to determine the most suitable torque trajectories of the clutches and engine, and the lower level control that manages the strategy for each actuator controller to track the given torque trajectories. The core of this study is the development of an effective upper level controller based on the optimal control allocation, to which previous studies have not paid adequate attention. A major advantage of this control approach is that the resulting shift performances can be easily and intuitively adjusted by tuning only one parameter. The effectiveness of the control scheme is demonstrated through various simulations using a high-fidelity DCT model implemented with a commercial software SimDriveline, and detailed discussions of the results are also provided.

1. Introduction

Recently, dual-clutch transmissions (DCTs) have garnered substantial attention in the global automotive industry because they have demonstrated significant improvements regarding both efficiency and ride quality of vehicles. During gear shifts, DCTs use two sets of clutches and transfer shafts to transmit the engine torque to the axle shaft without using torque converters, which can effectively nullify the drawbacks of other types of transmissions. In particular, such configurations enable the transmission systems to considerably reduce the torque discontinuities and interruptions, which are chronic problems in manual transmissions (MTs) and automated manual transmissions (AMTs); DCTs also result in significantly higher efficiency than conventional planetary-type automatic transmissions (ATs) do [1]. However, due to the absence of the smoothing effect of torque converters, DCT powertrains are more likely to cause awkward shift shocks during gear shifts, particularly when the clutch-to-clutch shift is performed fast [2]. Fast gear shifts are generally desired in order to minimize

* Corresponding author.
E-mail address: sbchoi@kaist.ac.kr (S. Choi).

http://dx.doi.org/10.1016/j.mechmachtheory.2017.02.013
0094-114X/

the loss of vehicle acceleration regardless of the transmission types. In addition, if the driver wants fast acceleration by pressing the accelerator pedal abruptly, the shift duration must be shortened accordingly [3]. In general, the conditions of comfortable and quick shifts conflict with each other and they are typically regarded as the two main objectives of gear shift controls (e.g. [4]).

The desired shift performances can only be attained when accompanied by precise torque transfer controls in vehicle drivelines. Various control strategies for gear shifts have been investigated for hydraulic ATs in [5–8]. Although the methodologies are similar to those for ATs, the lightly damped powertrains such as AMTs and DCTs need elaborate controls for the clutch(es) and engine throttle that focus more on ride quality improvement [3,9]. Shift control problems for AMTs have also been explored in numerous studies. Optimal linear quadratic clutch controllers were designed for dry AMTs considering several gear shifting performances in [10], and a clutch slip controller was developed to regulate the slip acceleration in [11]. In [12], a gear shift control strategy for an AMT was proposed through interpreting the gearshift process of AMTs as five phases considering its transient behaviors in each phase.

For DCT powertrains, however, gear shifts are realized through the handover of the torque delivered by the engine from one clutch to the other clutch, which further complicates the control problems. The DCT shifting process can be split into two phases: the torque phase where the torque is transferred from the engaged clutch to the on-coming clutch, and the inertia phase where the on-coming clutch with the new gear ratio is synchronized with the engine. In the torque phase, the cross shift control of the two clutches should be performed delicately in order to minimize the torque dip without causing an engine flare or clutch tie-up [7,13]. In the inertia phase, the synchronization control of the on-coming clutch accompanying the engine inertia control is crucial for comfortable ride quality and fast engagement. The engine throttle control is used to compensate the torque oscillations caused by the abrupt gear ratio change and the lag in the inertia torque [14,15]. Most literature on DCT shift control has adopted various methods of controlling torques or speeds in order to satisfy the pre-determined shift requirements in both phases [3,4,9,16,17]. The detailed control strategies of the clutch and engine speeds to meet the target torque requirement have been described in [3]. The gear shifts were divided into several phases and control strategies were proposed in each phase to ensure both fast and smooth clutch engagement based on the clutch slip and output torque information in [4]. A coordinated control algorithm for the engine and clutches to achieve the target average torque was proposed with detailed modeling of the hydraulic actuators in [9]. Since torque sensors are not available for production DCT powertrains, estimation methods for the torque states were developed in [18,19].

This paper proposes a new approach to the combined control of the clutches and engine throttle for a dry DCT gear shift considering the DCT driveline as an over-actuated system. A DCT has natural actuator redundancy because it has an additional clutch and shaft set compared with an AMT for the same transmission function. Previously, one of the clutches in a DCT or AT was controlled in an open-loop way so that it simply ramped up or down during the torque phase. There are several practical reasons for adopting this approach in these clutch-to-clutch shifts (see e.g. [7,16]), but the actuator redundancy problem must be addressed for more in-depth analysis of the shift processes. Here, the output shaft torque and the slip speed of the on-coming clutch are selected as the outputs to be controlled by the three actuators: the off-going clutch, the on-coming clutch, and the engine throttle. The control algorithm is divided into two levels: an upper level control that generates the desired torque values of each actuator considering the given shifting performances and a lower level control that forces on each actuator to follow the respective desired torque accurately.

A major shortcoming of previously published works is that there has been little research reported on the upper level control. Hence, this paper focuses on the development of a novel upper level controller that generates desired torque trajectories in real time for coordinated control of clutches and engine throttle using control allocation. Control allocation is a control technique for over-actuated systems that allocates the total control demand to the individual actuators [20,21]. Actuator redundancy can be found in various applications including the control of aerospace systems, marine vessels, and vehicles. Several control allocation approaches have been developed for vehicle motion control, such as vehicle yaw stabilization [22] and rollover prevention [23]. In this paper, the control allocator is designed to produce the optimized torque trajectories of two clutches and an engine after consideration of several actuator constraints. Using the proposed method, the desired torque trajectories can be designed to satisfy the shift requirements arbitrarily by tuning only one weighting factor between the two conflicting performances: fast shift and smooth shift. The resulting torque trajectories can be utilized as reference values for various shift control strategies, and they can also provide insights into the clutch-to-clutch shift process.

The remainder of this paper is organized as follows. In Section 2, DCT driveline and clutch actuator models are described. The DCT shift control structure consisting of the upper level and lower level controls is introduced, and detailed explanations of the developed control strategies are presented in Section 3. Next, in Section 4, the feasibility and effectiveness of the proposed control scheme are evaluated in simulations using a high-fidelity SimDriveline DCT model. A detailed discussion of the results is also presented. Finally, this study is concluded in Section 5.

2. System modeling

2.1. Driveline model

The basic configuration of the DCT is similar to that of an AMT, but the DCT is equipped with two sets of input and transfer shafts between the engine and the output shaft. The driveline model is composed of several angular speed dynamics

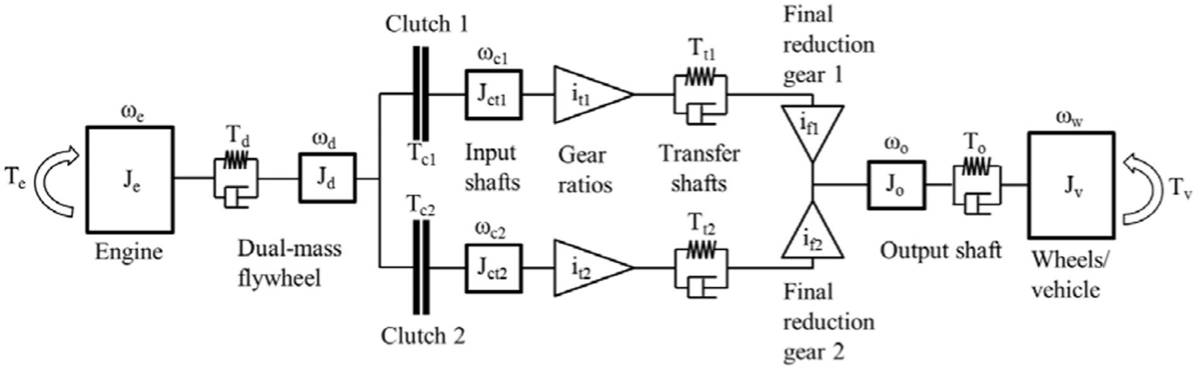

Fig. 1. Schematic of the DCT driveline.

based on the torque balance relationships for the lumped inertias of the individual components, as depicted in Fig. 1. J, T, ω, and θ are the inertia, torque, angular speed, and rotation angle, respectively. The subscripts e, d, $c1$, $c2$, $t1$, $t2$, o, w, and v refer to the engine, dual-mass flywheel, input shaft with clutch 1, input shaft with clutch 2, transfer shaft 1, transfer shaft 2, output shaft, wheel, and vehicle. The dynamics of the engine and dual-mass flywheel are expressed in Eqs. (1) and (2):

$$J_e\dot{\omega}_e = T_e - T_d, \tag{1}$$

$$J_d\dot{\omega}_d = T_d - T_{c1} - T_{c2}, \tag{2}$$

where the engine torque is a function of the throttle position and engine speed, i.e. $T_e = f(\alpha_{th}, \omega_e)$.

The torsional compliance caused by the dual-mass flywheel is modeled in Eq. (3):

$$T_d = k_d(\theta_e - \theta_d) + b_d(\omega_e - \omega_d), \tag{3}$$

where k_d and c_d are the torsional stiffness and damping coefficient of the dual-mass flywheel, respectively.

The compliance of the dual-mass flywheel is often ignored in simplified control-oriented models because measuring its angular speed and torque accurately is not possible in production DCTs. In this case, the total inertia of the engine and dual-mass flywheel is regarded as one lumped engine inertia.

In the same manner, defining the equivalent inertias from clutch 1 and clutch 2 perspectives for the masses including the input and transfer shafts, gears, and synchronizers as J_{ct1} and J_{ct2}, respectively, the dynamics of each transfer shaft is described in Eqs. (4) and (5), as follows:

$$J_{ct1}\dot{\omega}_{c1} = T_{c1} - \frac{T_{t1}}{i_{t1}}, \tag{4}$$

$$J_{ct2}\dot{\omega}_{c2} = T_{c2} - \frac{T_{t2}}{i_{t2}}, \tag{5}$$

where i_{t1} is the gear ratio of the input and transfer shaft 1, and i_{t2} is that of the input and transfer shaft 2.

The torque transmitted through each clutch is modeled in Eqs. (6) and (7) depending on the states of the clutches: disengaged, slipping, and engaged [24].

$$T_{c1} = \begin{cases} 0 & \text{if disengaged} & \\ \mu_{k1}F_{n1}r_{c1}N_1D_1\,\mathrm{sgn}(\omega_d - \omega_{c1}) & \text{if } |\omega_d - \omega_{c1}| \geq \varepsilon_{tol} & \text{(slipping)} \\ T_{in1} \triangleq T_d - T_{c2} - J_d\dot{\omega}_d & \text{if } |\omega_d - \omega_{c1}| < \varepsilon_{tol} \text{ and } T_{c1,\max} \geq |T_{in1}| & \text{(engaged)} \\ \mu_{k1}F_{n1}r_{c1}N_1D_1\,\mathrm{sgn}(T_{in}) & \text{if } |\omega_d - \omega_{c1}| < \varepsilon_{tol} \text{ and } T_{c1,\max} < |T_{in1}| & \text{(slipping)} \end{cases}$$
$$\text{where } T_{c1,\max} = \mu_{s1}F_{n1}r_{c1}N_1D_1 \tag{6}$$

$$T_{c2} = \begin{cases} 0 & \text{if disengaged} & \\ \mu_{k2}F_{n2}r_{c2}N_2D_2\,\mathrm{sgn}(\omega_d - \omega_{c2}) & \text{if } |\omega_d - \omega_{c2}| \geq \varepsilon_{tol} & \text{(slipping)} \\ T_{in2} \triangleq T_d - T_{c1} - J_d\dot{\omega}_d & \text{if } |\omega_d - \omega_{c2}| < \varepsilon_{tol} \text{ and } T_{c2,\max} \geq |T_{in2}| & \text{(engaged)} \\ \mu_{k2}F_{n2}r_{c2}N_2D_2\,\mathrm{sgn}(T_{in2}) & \text{if } |\omega_d - \omega_{c2}| < \varepsilon_{tol} \text{ and } T_{c2,\max} < |T_{in2}| & \text{(slipping)} \end{cases}$$
$$\text{where } T_{c2,\max} = \mu_{s2}F_{n2}r_{c2}N_2D_2 \tag{7}$$

In Eqs. (6) and (7), μ_k, μ_s, F_n, r_c, N, and D are the kinetic, static friction coefficients, and actuator normal force, effective torque radius, number of friction surfaces, and de-rating factor of each clutch, respectively. The clutch state is determined by the magnitude of its slip speed and by the comparison of its maximum torque capacity ($T_{c,\max}$) and the input torque to the clutch delivered from the flywheel T_{in}.

The speed dynamics of the output shaft and wheel are also described using the principle of torque balance, as described in Eqs. (8) and (9).

$$J_o\dot{\omega}_o = i_{f1}T_{t1} + i_{f2}T_{t2} - T_o, \tag{8}$$

$$J_v\dot{\omega}_w = T_o - T_v, \tag{9}$$

where T_v is the vehicle load torque, which includes the rolling resistance, road gradient, and aerodynamic drag. The output shaft torque (T_o) can be modeled using the torsional compliance model in the same manner as the dual-mass flywheel, as described in Eq. (10):

$$T_o = k_o(\theta_o - \theta_w) + b_o(\omega_o - \omega_w), \tag{10}$$

where k_o and c_o are the torsional stiffness and damping coefficient of the output shaft, respectively.

2.2. Clutch actuator model

The base dry DCT for this work is equipped with electric actuators designed using the self-energizing mechanism. The actuators are characterized by their high efficiency because the self-energizing mechanism uses the energy acquired from the frictional losses dissipated in the clutch in order that the required power for the actuation is significantly reduced. The self-energizing mechanism of the actuator results from its unique mechanical structure attached to a conventional DC motor. A full explanation of the working principles and advantages of this actuator is out of scope; therefore, only a brief introduction is provided in this section. For more information, refer to [25,26]. Here, only the dynamics of the actuators for the lower level controller implementation are discussed. The governing equations for the self-energizing actuation motor during the clutch engagement/disengagement are presented in Eq. (11) for the mechanical section and Eq. (12) for the electrical section.

$$J_a\dot{\omega}_m = T_m - \frac{T_c}{N_{ae}} - \frac{2r_p \tan\alpha}{N_{ae}} - T_f, \tag{11}$$

where α, r_p, and N_{ae} are the constants determined by the geometry of the actuator, and ω_m, T_m, and T_f indicate the angular speed, driven torque of the motor, and net friction torque in the actuator route, respectively.

$$\begin{aligned} &L_m\frac{di_m}{dt} = -k_e\omega_m - R_m i_m + V_{in}, \\ &T_m = k_t i_m, \end{aligned} \tag{12}$$

where L_m, k_e, k_t, R_m, V_{in}, and i_m are the motor inductance, back-emf constant, torque constant, armature resistance, control input, and motor current, respectively.

3. Control methodology

3.1. Overview and objectives

This paper proposes a novel strategy for the coordinated control of the clutches and engine throttle of DCTs via control allocation. Here, the strategy is developed for the 1-2 upshift in a dry DCT. The goal of the DCT shift control is to perform the clutch-to-clutch shift as fast as the driver's intention while satisfying the ride quality criteria without causing clutch tie-up or engine flare. A clutch tie-up occurs if excessive torque capacity is added to the on-coming clutch while the off-going clutch has torque holding capacity. An engine flare results when the off-going clutch is released too early and the on-coming clutch does not have sufficient torque capacity to hold the engine torque at that time [27,28]. Thus, in order to meet the given shift requirements, sophisticated control of both the transmitted torque and the torque capacity of each clutch is crucial. As described in Eqs. (6) and (7), the torque capacity of the clutch determines the clutch state, i.e. whether it is engaged or slipping. Both the torque capacity (of an engaged clutch) and the torque (transmitted through a slipping clutch) are directly related to the corresponding forces (pressure) on the clutches, which are determined by the positions of each clutch actuator. Hence, the shift control algorithm is designed to consist of two level controls, as depicted in Fig. 2. The upper level controller assigns the optimized reference torque trajectories of the two clutches and the engine regarding the desired shift performances. Then, the lower level controller attempts to track the given torque trajectories considering the dynamics of the actuators.

Once the gear shift (upshift) is initiated, the torque phase where the torque handover occurs from the off-going clutch to the on-coming clutch begins immediately. In the torque phase, poor clutch control results in undesirable shift responses that possibly accompany clutch tie-up, engine flare, or torque oscillations caused by stick-slip transitions. The force on the off-going clutch should be gradually decreased in order to reduce its torque capacity while the on-coming clutch force is increased to ensure a smooth torque transfer with minimal torque dip [9]. Furthermore, the torque capacity of the off-going clutch should be above its transmitted torque for as long as the on-coming clutch is slipping during the torque phase [17]. When the off-going clutch starts to slip, the inertia phase begins. At the beginning of the inertia phase, both clutches are slipping until the off-going clutch is completely disengaged. It is desired that the off-going clutch should be fully disengaged

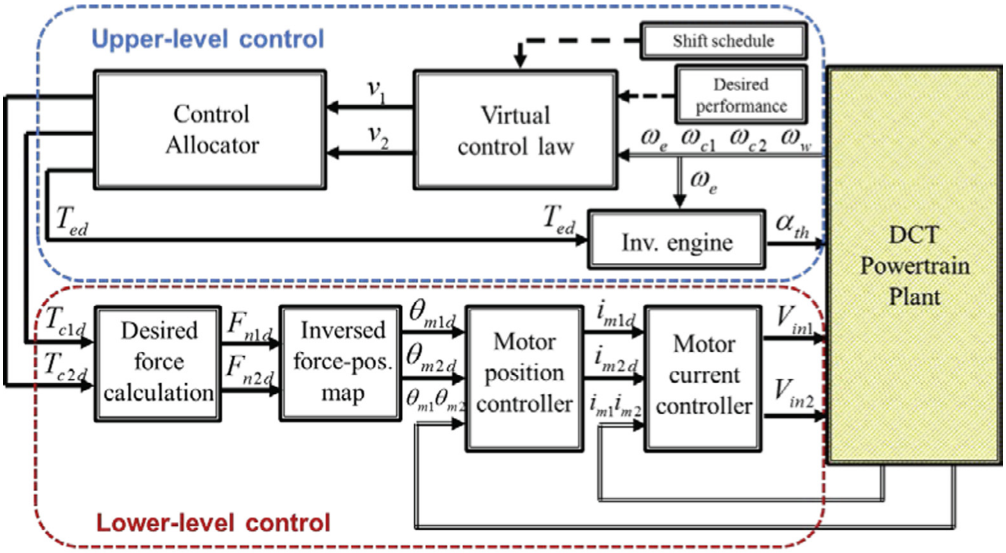

Fig. 2. Control structure.

at the precise moment that the transmitted torque through it becomes zero [7]. After the off-going clutch is disengaged, the control methodologies of clutch engagement originally designed for AMTs can be directly applied. In order to ensure smooth and fast engagement of the on-coming clutch with the new gear, the slip acceleration or output shaft torque as well as its slip speed should be appropriately regulated by the clutch actuator control integrated with the engine throttle manipulation [4,11,12,16]. In addition, it is also important to reduce the frictional energy dissipated in the clutch for durability.

3.2. Control allocation concept

A key objective of this work is to develop an effective control allocator as part of the upper level control that generates the optimized torque trajectories of the individual clutches and engine during gear shifts. The concept of the control allocation is briefly introduced in this sub-section. Control allocation is an effective control method for over-actuated systems in order to distribute the total control demand into each actuator. Basic linear control allocation problems can be simply expressed as in Eq. (13) [20]:

$$\begin{aligned} &Bu(t) = v(t), \\ &u_{\min} \le u(t) \le u_{\max}, \end{aligned} \tag{13}$$

where $v(t) \in \mathbb{R}^k$ is the virtual control input representing the total control demand, $u(t) \in \mathbb{R}^m$ is the actual control input, and B is the control effectiveness matrix that defines the relationships of u and v. The actuator constraints of u, including its rate constraints, are set by assigning appropriate values to $u_{\min}$ and $u_{\max}$. For over-actuated systems, $m > k$ should be satisfied. The objective of the control allocation is to determine the constrained actual input $u(t)$ that satisfies Eq. (13) provided that the virtual input ($v(t)$) is designed in advance. In this paper, the optimal control allocation using weighted least squares (WLS) is utilized for the DCT control; the WLS method is well known for its faster computation time compared with other methods, and it can be formulated as follows:

$$u_{CA} = \arg \min_{u_{\min} \le u \le u_{\max}} (\|W_u(u - u_r)\|^2 + \gamma \|W_v(Bu - v)\|^2), \tag{14}$$

where u_r is the reference actual input, and γ, W_u, and W_v are weighting factors.

Eq. (14) calculates the optimized feasible input u_{CA} that minimizes $u - u_r$ and $Bu - v$ simultaneously in accordance with the weighting factors γ, W_u, and W_v. The weighting factor γ is typically chosen as a very large value to express the priority of minimizing $\|W_v(Bu - v)\|^2$.

Such constrained optimization problems can be solved in real time using active set method [20, 23]. The active set method finds approximate solutions to the problems with high precision that are suitable for real time applications. The detailed algorithm of it used in this work is described in the appendix [20].

3.3. Upper level control law

3.3.1. Equation formulation

Assuming that the compliance of the dual-mass flywheel is negligible, Eqs. (1) and (2) are combined in Eq. (15).

$$J_{e+d}\dot{\omega}_e = T_e - T_{c1} - T_{c2},\quad \text{where } J_{e+d} \triangleq J_e + J_d. \tag{15}$$

Also, rearranging Eqs.(4) and (5) to isolate T_{t1} and T_{t2}, respectively, results in Eqs.(16) and (17) being derived.

$$T_{t1} = i_{t1}(T_{c1} - J_{ct1}\dot{\omega}_{c1}), \tag{16}$$

$$T_{t2} = i_{t2}(T_{c2} - J_{ct2}\dot{\omega}_{c2}). \tag{17}$$

Substituting Eqs. (16) and (17) into Eq. (8) and then combining with Eq. (15), the following expression of output shaft torque is obtained.

$$T_o = (i_{t1}i_{f1} - 1)T_{c1} + (i_{t2}i_{f2} - 1)T_{c2} + T_e - i_{t1}i_{f1}J_{ct1}\dot{\omega}_{c1} - i_{t2}i_{f2}J_{ct2}\dot{\omega}_{c2} - J_o\dot{\omega}_o - J_{e+d}\dot{\omega}_e. \tag{18}$$

Finally, using the methodology investigated in [29], Eq. (18) is simplified by the reduced-order approximations in each phase:

$$T_o = \begin{cases} (i_{t1}i_{f1} - 1)T_{c1} + (i_{t2}i_{f2} - 1)T_{c2} + T_e - J_{o,eq}\dot{\omega}_{c1} & \text{(torque phase)} \\ (i_{t1}i_{f1} - 1)T_{c1} + (i_{t2}i_{f2} - 1)T_{c2} + T_e - (J_{o,eq} - J_{e+d})\dot{\omega}_{c1} - J_{e+d}\dot{\omega}_e & \text{(inertia phase)} \end{cases}$$
$$\text{where } J_{o,eq} \triangleq i_{t1}i_{f1}J_{ct1} + \frac{(i_{t2}i_{f2})^2}{i_{t1}i_{f1}}J_{ct2} + \frac{1}{i_{t1}i_{f1}}J_o + J_{e+d} \tag{19}$$

Next, through manipulating the above equations, the slip dynamics of the on-coming clutch are easily derived as described in Eq. (20) assuming $\frac{\omega_{c1}}{i_{t1}i_{f1}} = \omega_o$ during the inertia phase.

$$\begin{aligned} \dot{\omega}_{sl2} &= \dot{\omega}_e - \dot{\omega}_{c2} \\ &= \frac{1}{J_{e+d}}(T_e - T_{c1} - T_{c2}) - \frac{1}{i_{t2}i_{f2}J_{ct2}}(i_{t1}i_{f1}T_{c1} + i_{t2}i_{f2}T_{c2} - i_{t1}i_{f1}J_{ct1}\dot{\omega}_{c1} - T_o - J_o\dot{\omega}_o) \\ &= \frac{1}{J_{e+d}}T_e - \left(\frac{1}{J_{e+d}} + \frac{i_{t1}i_{f1}}{i_{t2}i_{f2}J_{ct2}}\right)T_{c1} - \left(\frac{1}{J_{e+d}} + \frac{1}{J_{ct2}}\right)T_{c2} + J_{sl2,eq}\dot{\omega}_{c1} + \frac{T_o}{i_{t2}i_{f2}J_{ct2}} \\ &\quad \text{where } J_{sl2,eq} \triangleq \frac{i_{t1}i_{f1}J_{ct1} + \frac{1}{i_{t1}i_{f1}}J_o}{i_{t2}i_{f2}J_{ct2}} \end{aligned} \tag{20}$$

Examining Eqs. (19) and (20), it is apparent that both the output torque and the slip speed are not governed by one particular actuator. Hence, the lumped virtual inputs are derived for the output variables, and then the lumped control demands are distributed in the actual control inputs instead of developing decentralized control laws for each output directly. The virtual inputs v_1 and v_2 are defined as follows:

$$\begin{aligned} v_1 &\triangleq (i_{t1}i_{f1} - 1)T_{c1} + (i_{t2}i_{f2} - 1)T_{c2} + T_e \\ v_2 &\triangleq -\left(\frac{1}{J_{e+d}} + \frac{i_{t1}i_{f1}}{i_{t2}i_{f2}J_{ct2}}\right)T_{c1} - \left(\frac{1}{J_{e+d}} + \frac{1}{J_{ct2}}\right)T_{c2} + \frac{1}{J_{e+d}}T_e, \end{aligned} \tag{21}$$

which are the two virtual inputs to regulate the output shaft torque and the slip speed, respectively. Here, T_{c1}, T_{c2}, and T_e are the actual inputs generated by the actuators that should be allocated. Using the matrix representation of Eq. (13), the relationship of the actual and virtual inputs is expressed as described in Eq. (22):

$$\vec{v} = \begin{bmatrix} v_1 \\ v_2 \end{bmatrix} = B\vec{u} = \begin{bmatrix} i_{t1}i_{f1} - 1 & i_{t2}i_{f2} - 1 & 1 \\ -\left(\frac{1}{J_{e+d}} + \frac{i_{t1}i_{f1}}{i_{t2}i_{f2}J_{ct2}}\right) & -\left(\frac{1}{J_{e+d}} + \frac{1}{J_{ct2}}\right) & \frac{1}{J_{e+d}} \end{bmatrix} \begin{bmatrix} T_{c1} \\ T_{c2} \\ T_e \end{bmatrix}. \tag{22}$$

3.3.2. Virtual control laws

The design procedure of the upper level controller occurs in two steps. First, assuming that two virtual actuators whose control effects are represented as v_1 and v_2 exist, the control laws for the virtual inputs to effectively regulate T_o and ω_{sl2} are derived; second, the control allocation algorithm is developed to distribute the virtual control demands of v_1 and v_2 into the feasible actual control inputs of u_1, u_2, and u_3. Although this study focuses on the clutch-to-clutch shift control of DCTs, this methodology can also be applied to gear shift controls of conventional hydraulic ATs.

Because the output shaft torque is generally not measurable in production transmissions, a feed forward control law is adopted to control it in order to track the demanded output torque. If the desired output torque trajectory T_{od} is given throughout the gear shift, the required v_1 value is calculated for each phase using Eq. (19). Thus, the first virtual control law is derived, as described below.

$$v_{1d} \triangleq \begin{cases} T_{od} + J_{o,eq}\dot{\omega}_{c1} & \text{(torque phase)} \\ T_{od} + (J_{o,eq} - J_{e+d})\dot{\omega}_{c1} + J_{e+d}\dot{\omega}_e & \text{(inertia phase)}. \end{cases} \tag{23}$$

Next, the second virtual control law that regulates the on-coming clutch slip is designed based on Eq. (20), as follows:

$$v_{2d} \triangleq -J_{sl2,eq}\dot{\omega}_{c1} - \frac{T_o^d}{i_{t2}i_{f2}J_{ct2}} - \lambda_P\omega_{sl2} - \lambda_D\dot{\omega}_{sl2}, \tag{24}$$

where λ_P, λ_D are proportional and derivative gains.

v_{2d} is found in the form of a proportional derivative slip controller with feed forward terms that reflect the effects of the inertia torque and desired output torque. Once the off-going clutch begins to slip (inertia phase), v_2 is activated.

3.3.3. Control allocator design

The strategies of the control allocation for the power-on upshift from 1 to 2 are implemented, as follows.

(i) The desired output torque trajectory is a smooth trajectory consisting of steady state values for the output torque of the 1st and 2nd gears without torque dip and lock up oscillation.

(ii) The concept of the reference actual inputs $\vec{u}_r = [u_{1r} \quad u_{2r} \quad u_{3r}]^T$ is introduced in the optimal control allocation in Eq. (14) so that if there are many solutions for u_{1CA}, u_{2CA}, and u_{3CA} that satisfy $B\vec{u} = \vec{v}$, the WLS algorithm selects the closest ones to u_{1r}, u_{2r}, and u_{3r}. Here, the reference inputs are defined as follows:

$$\begin{aligned} u_{1r}(k) &\triangleq u_{1CA}(k-1) + \{u_{1CA}(k-1) - u_{1CA}(k-2)\}, \\ u_{2r}(k) &\triangleq u_{2CA}(k-1) + \{u_{2CA}(k-1) - u_{2CA}(k-2)\}, \\ u_{3r}(k) &\triangleq T_{e,n}(k), \end{aligned} \tag{25}$$

where $u_{1CA}(k-n)$ and $u_{2CA}(k-n)$ are the allocated clutch torque inputs with n-step delays obtained from Eq. (14), and $T_{e,n}(k)$ is the nominal engine torque, with $T_{e,n} = T_{e,n}(\alpha_{th}, \omega_e)$ determined by the driver's pedal position. Eq. (25) implies that the rate change of each clutch torque should be as small as possible in order to reduce the unwanted torque oscillations (u_{1r}, u_{2r}), and as the discrepancy between the controlled engine torque and the nominal engine torque decreases, the driving feel is improved (u_{3r}).

(iii) The actuator constraints and its rate constraints are as follows.

(1) The signs of the rates of the clutch torques should not be changed, which means that the off-going clutch should always move in the direction that its torque is decreasing and that the on-coming clutch should move in the opposite way, i.e. $\dot{u}_1 \le 0,\ \dot{u}_2 \ge 0$, in order to ensure a smooth cross-shift [30].

(2) The clutch torque values should not have negative values to prevent clutch tie-up and to avoid backward power recirculation, i.e. $u_1 \ge 0$, $u_2 \ge 0$.

(3) The torque transmitted through a clutch should always be smaller than its torque capacity and the effective input torque delivered from the engine, i.e. $u_1 \le \min(T_{in1},\ T_{c1\_\max}),\ u_2 \le \min(T_{in2},\ T_{c2\_\max})$.

(4) The rates of torques are constrained by the bandwidths of the corresponding clutch actuators and engine, $|\dot{u}_1| \le \rho_1,\ |\dot{u}_2| \le \rho_2,\ |\dot{u}_3| \le \rho_3$.

(5) The engine throttle control is only activated in the inertia phase, i.e.

$$u_3 = \begin{cases} T_{ed} \text{ in inertia phase} \\ T_{e,n} \text{ otherwise} \end{cases},$$

where T_{ed} is the engine torque input determined by the control allocator.

(6) The engine speed must be above its minimum value during a gear shift in order to avoid stalling, which is also referred to as the "no-kill condition", $\omega_e \ge \omega_{e,\min}$ [12,31].

Then, the control allocator calculates the feasible combinations of u_{1CA}, u_{2CA}, and u_{3CA} using Eq. (14) based on the allocation strategies. In this study, fixed values are assigned to W_u and γ such that $W_u = I_{3\times3}$ and $\gamma = 10^5$. Then, through adjusting only W_v freely (weighting between v_1 for a fast gear shift and v_2 for a comfortable gear shift), the optimized torque trajectories of the clutches and engine with different performances are produced.

One advantage of using optimal control allocation in DCT shift controls is that it considers the pre-determined constraints of actuators in real time. For example, when a clutch is engaged, the control allocator assumes that the corresponding clutch torque is constrained by the other torque inputs or if it is disengaged, the corresponding clutch input is regarded to be saturated to zero. Such constraints play a key role to determine the most feasible combination of u_{1CA}, u_{2CA}, and u_{3CA}.

3.4. Lower level control

The torque tracking controllers for both clutch actuators and the engine are developed after consideration of the actuators' dynamics. For the clutches, the reference torque trajectories given from the upper level controller should be converted to the corresponding forces and actuator positions for the lower level controller to track. Because the actuation force or pressure information is not available as it is for hydraulic actuation, the force characteristic maps, which are experimentally obtained, are used. Since designing a novel lower level controller with high tracking performance is not an objective of this study, a detailed discussion on the uncertainty of the force-position map is omitted. For more details, see [32,33] where the effects of thermal expansion and clutch wear on the torque transmissibility of a dry clutch were well investigated. Another requirement of the lower level control is that the controlled response should track the reference torque values sufficiently fast in order that the upper level control law can be tuned independently from the lower level control [34].

3.4.1. Engine throttle control

The engine throttle control is only in effect in the inertia phase. While the desired engine torque (u_{3CA}) is computed from the upper level controller, the torque values are immediately converted to the corresponding engine throttle positions via the inversed engine model according to the current engine speed. Here, the first order dynamic equation is used to describe the engine dynamics as (26).

$$\tau_e \dot{T}_{e\_lag} + T_{e\_lag} = T_{ed} \tag{26}$$

where τ_e and T_{e_lag} are time constant and lagged torque response of the engine.

The inversed engine model consists of the inversed engine dynamics and the inversed static engine map. The calculated throttle position is processed with a low pass filter in order to attenuate its unrealistic high frequency components. During the inertia phase, the slip speed of the on-coming clutch and the output torque response are adjusted using the engine control in conjunction with the on-coming clutch control. Once the synchronization is completed, the engine throttle position returns to its initial value at the beginning of the inertia phase.

3.4.2. Control of clutch actuators

3.4.2.1. Desired clutch force trajectories. Examining Eqs. (6) and (7), if the clutch is in the slipping phase, the relationship of the transmitted torque and the clutch force is prescribed by the Coulomb friction equation. However, when the clutch is in the engaged phase, the transmitted torque through it is unrelated to the normal force on it. Instead, the normal force on the engaged clutch affects the clutch torque capacity. During the majority of the torque phase, the off-going clutch is engaged and the on-coming clutch is slipping. Given the reference clutch torque values for both clutches, denoted as T_{c1d} and T_{c2d}, the following strategy to obtain their force trajectories is adopted:

$$\begin{aligned} F_{n1d} &= \frac{T_{c1d}}{\gamma_{c1}\mu_{s1} r_{c1} N_1 D_1}, \\ F_{n2d} &= \frac{T_{c12}}{\mu_{k1} r_{c2} N_2 D_2}. \end{aligned} \tag{27}$$

where γ_{c1} is a margin factor for the engaged clutch control such that $0 < \gamma_{c1} < 1$.

For the on-coming clutch, the corresponding force values are easily calculated using the kinetic Coulomb friction model. For the off-going clutch, its torque capacity should be maintained above its input torque from the engine side in order that the clutch is not released too early during the torque phase. Furthermore, its normal force is desired to be zero immediately after the transmitted torque becomes zero. Through adding the margin factor γ_{c1} to the static friction equation, the force trajectory that satisfy these requirements are generated. The theory behind the inclusion of the margin factor γ_{c1} is to keep $T_{c1,\max}$ above T_{c1} during the torque phase, and to make $T_{c1,\max} = 0$ at the precise moment when $T_{c1} = 0$ by letting $F_{n1} = 0$. Note that it is assumed that the friction coefficients vary slowly in order that they are regarded as constants during the gear shift. For a detailed discussion on the dynamic friction coefficient model, see [35].

3.4.2.2. Control laws. The electrical section of the actuator is a simple DC motor. Considering the characteristics of its dynamics and also the aforementioned requirements of lower level control, simple PD position tracking controllers are developed for both clutch actuators, as described in the following two sets of equations.

$$\begin{aligned} &i_{m1d} \triangleq -\lambda_{p1} e_{m1} - \lambda_{d1} \dot{e}_{m1} \\ &i_{m2d} \triangleq -\lambda_{p2} e_{m2} - \lambda_{d2} \dot{e}_{m2} \\ &\text{where } e_{m1} \triangleq \theta_{m1} - \theta_{md1}, \;\; e_{m2} \triangleq \theta_{m2} - \theta_{md2} \end{aligned} \tag{28}$$

$$\begin{aligned} V_{in1} &= L_{m1} \frac{di_{m1d}}{dt} + k_{e1}\omega_{m1} + R_{m1} i_{m1d} \\ V_{in2} &= L_{m2} \frac{di_{m2d}}{dt} + k_{e2}\omega_{m2} + R_{m2} i_{m2d} \end{aligned} \tag{29}$$

In Eq. (28), θ_{m1}, θ_{m2}, θ_{md1}, θ_{md2} are actual and desired positions of each clutch actuator, and λ_{p1}, λ_{p2}, λ_{d1}, λ_{d2} stand for proportional and derivative gains for each controller.

Table 1
System parameters.

		Vehicle parameters
$J_e = 0.2$	$k_o = 9520$	
$J_d = 0.086$	$b_o = 591$	vehicle mass : 1600
$J_{ct1} = 0.0577$	$i_{t1} = 3.688$	tire rolling resistance coefficient : 0.015
$J_{ct2} = 0.0355$	$i_{t2} = 2.580$	aerodynamic drag coefficient : 0.4
$J_o = 0.04$	$i_{f1} = i_{f2} = 4.119$	frontal area : 3
$k_d = 215$	$r_{c1} = r_{c2} = 0.13$	wheel radius : 0.312
$b_d = 10$	$N_1 = N_2 = 4$	road inclination : 0
$k_{t1} = 15420$	$D_1 = D_2 = 1$	
$b_{t1} = 53$	$\mu_{k1} = \mu_{k2} = 0.27$	[units are SI derived
$k_{t2} = 15000$	$\mu_{s1} = \mu_{s2} = 0.30$	(kg, N, rad, m, s, A)]
$b_{t2} = 51$	$J_w = 1.7747$	

Table 2
Shift performance comparison (*: best value).

	Peak vehicle acc. (m/s^2)	Peak vehicle jerk (m/s^3)	Torque dip $T_o(t_i) - T_{o,\min\_TP}$ (Nm)	Shift time $t_f - t_i$ (s)	Frictional loss E_d (J)
Case 1	1.795*	13.1*	96.3*	0.691	2224
Case 2	2.735	21.7	96.3*	0.476*	1740*
Case 3	2.452	19.11	96.3*	0.514	1850

4. Simulations and discussions

Several simulations were conducted for different values of W_v in order to verify the effectiveness of the proposed method. The DCT powertrain model was implemented using SimDriveline, which is a high-fidelity simulation tool appropriate for modeling and simulating vehicle transmission systems. Other vehicle components including the engines and tires, as well as

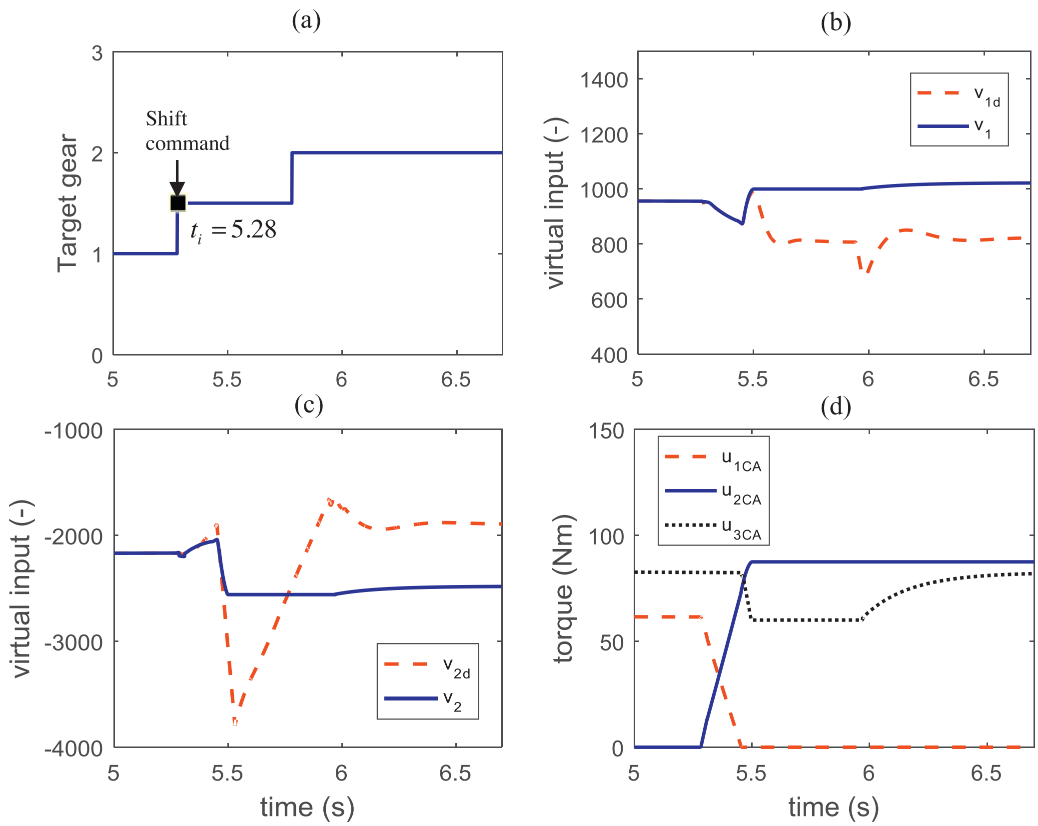

Fig. 3. Upper level control for Case 1 ($W_v = [10\ 0; 0\ 1]$): (a) target gear, (b) virtual input 1, (c) virtual input 2, and (d) resulting allocated torques.

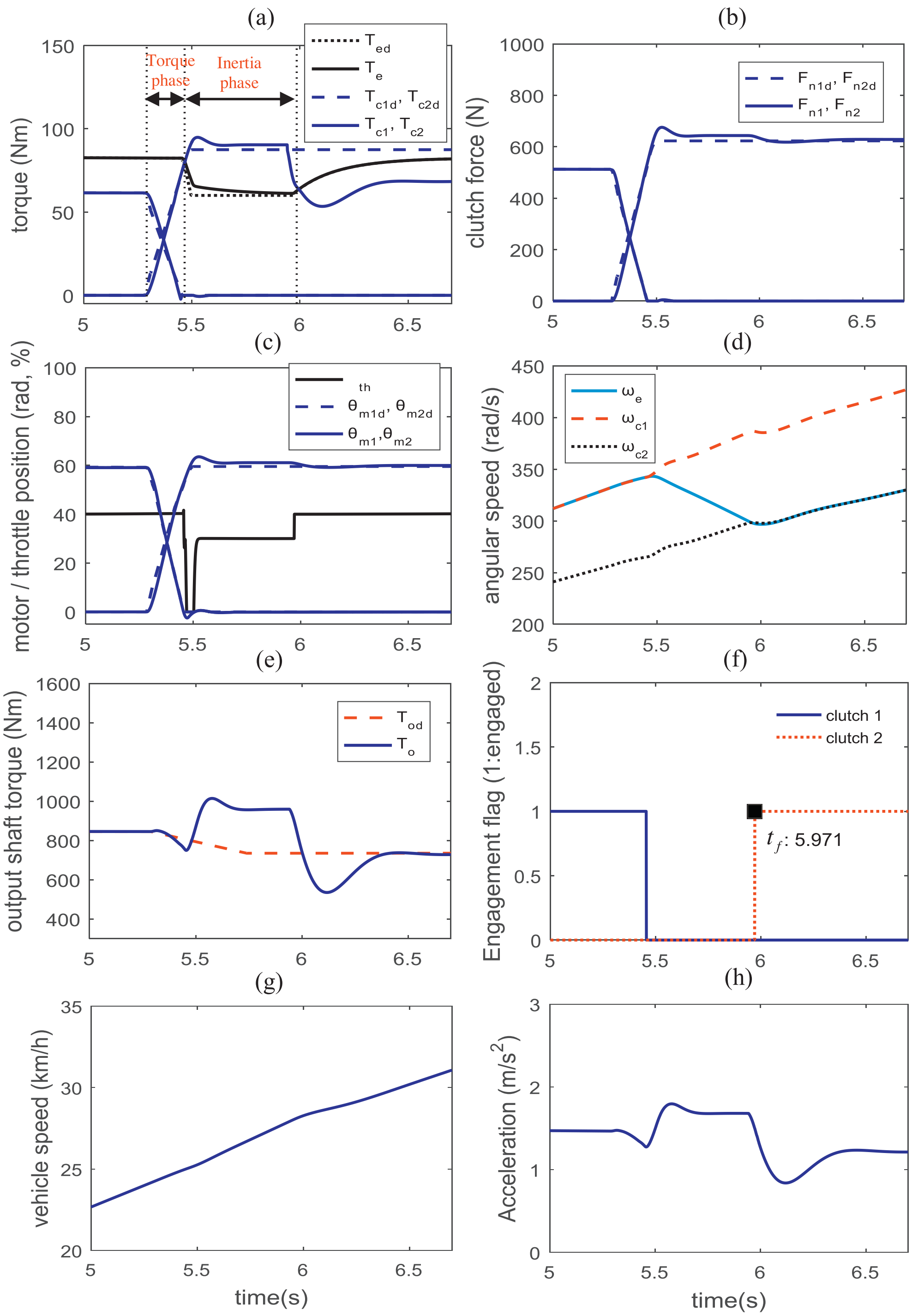

Fig. 4. Lower level control for Case 1 ($W_v = [10\ 0; 0\ 1]$): (a) torque, (b) clutch force, (c) actuator position, (d) speed, (e) output torque, (f) engagement flag, (g) vehicle speed, and (h) vehicle acceleration.

the basic mechanical parts, are also accurately modeled using SimDriveline for realistic simulations. The parameters of the transmission used for the simulations are provided in Table 1.

Note that v_1 is the first virtual input for the output torque tracking control, while v_2 is the second virtual input for the fast slip control. In the WLS algorithm (14), W_v is a 2×2 diagonal matrix that determines the relative weighting between v_1 and v_2 during the control allocation process. The feasibility of the developed control strategy is demonstrated through

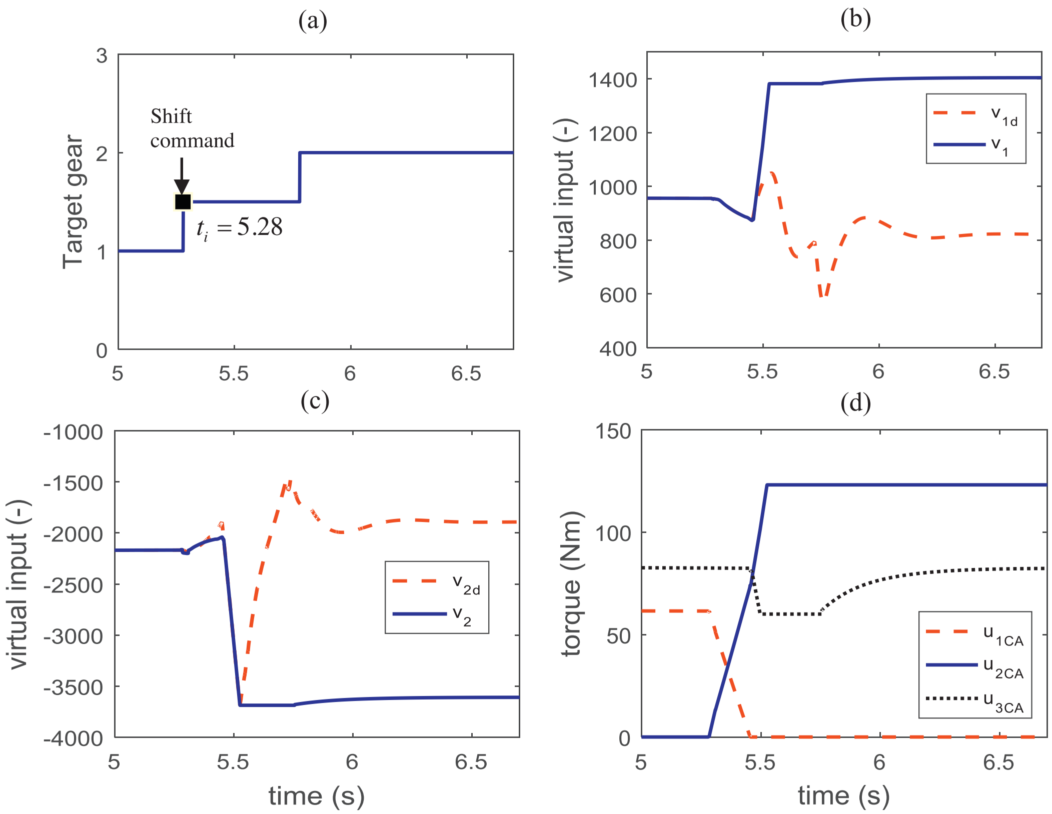

Fig. 5. Upper level control for Case 2 ($W_v = [1\ 0; 0\ 10]$): (a) target gear, (b) virtual input 1, (c) virtual input 2, and (d) resulting allocated torques.

comparing the simulation results obtained by assigning three different W_v values in each simulation (the other weighting factors are fixed, i.e. $W_u = I_{3\times3}$ and $\gamma = 10^5$).

Case 1: $W_v = [10\ 0; 0\ 1]$

In Case 1, the control allocator should generate the desired torques in order to ensure better tracking performance of v_1 than that of v_2. The results of the upper level control and lower level control are depicted in Figs. 3 and 4, respectively.

The gear shift is initiated at 5.28 s, and the virtual control law v_1 is activated immediately. v_2 comes into effect with the start of the inertia phase. Because v_1 is weighted more than v_2, it is seen that the tracking performance of v_1 is significantly better during the shift. Thus, a comfortable shift with a smooth acceleration is expected as a result of the upper level control strategy. After approximately 5.5 s, the actual v_1 and v_2 cannot follow the desired values well due to the physical actuator constraints defined in the previous section. Fig. 3(d) presents the resulting torque trajectories given by the control allocator. During the control allocation, the clutch torque values are guided by u_{1r} and u_{2r} using the WLS algorithm to minimize the rate change of the torques. The torque trajectories are used as the reference values for lower level control of the engine and clutches.

While the clutch torques tracked the reference torques well without clutch tie-up or fluctuation, the engine had slightly lagged responses due to its inertia effects (Fig. 4(a)). The cross shift of both clutches is realized in order that the torque is smoothly transferred from the off-going clutch to the on-coming clutch in order to reduce the shift impact. In detail, during the torque phase, the force of the on-coming clutch is gradually increased while the off-going clutch force is reduced to decrease its torque capacity aligning with the on-coming clutch torque in order to avoid clutch tie-ups and engine flares. It is seen that the torque dip and the corresponding loss of acceleration are very small (Fig. 4(e) and (h)). When the inertia phase begins, the force (or actuator position) of the on-coming clutch is increased further, but remained at a relatively low value to minimize the overshoot of the output torque (Fig. 4(b) and (e)). In the inertia phase, the engine throttle controller is switched on and assists with the synchronization between the on-coming clutch and the flywheel through reducing its torque while the torque of the on-coming clutch is maintained at a low value ($<$100 Nm). Finally, the lock-up of the on-coming clutch is achieved smoothly, and then the torque transmitted through it is reduced to near the engine torque with the second gear. As a result, the overshoot and oscillation of the on-coming clutch torque are also relatively small during the shift, thereby leading to small peak values and slight fluctuations of the output torque and vehicle acceleration (Fig. 4(e) and (h)). However, the shift time is increased slightly due to the slow engagement of the on-coming clutch (Fig. 4(d) and

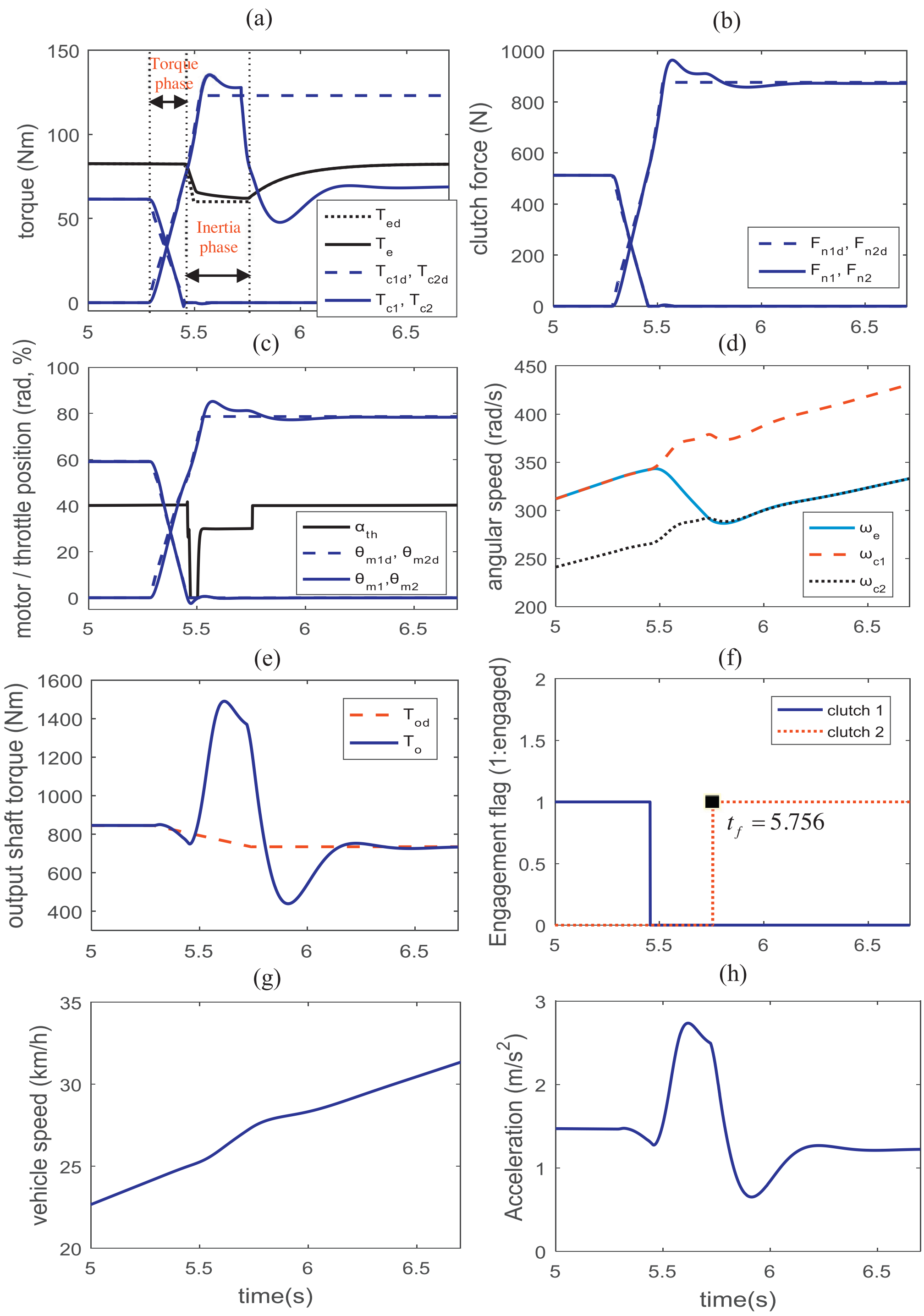

Fig. 6. Lower-level control for Case 2 ($W_v = [1\ 0; 0\ 10]$): (a) torque, (b) clutch force, (c) actuator position, (d) speed, (e) output torque, (f) engagement flag, (g) vehicle speed, and (h) vehicle acceleration.

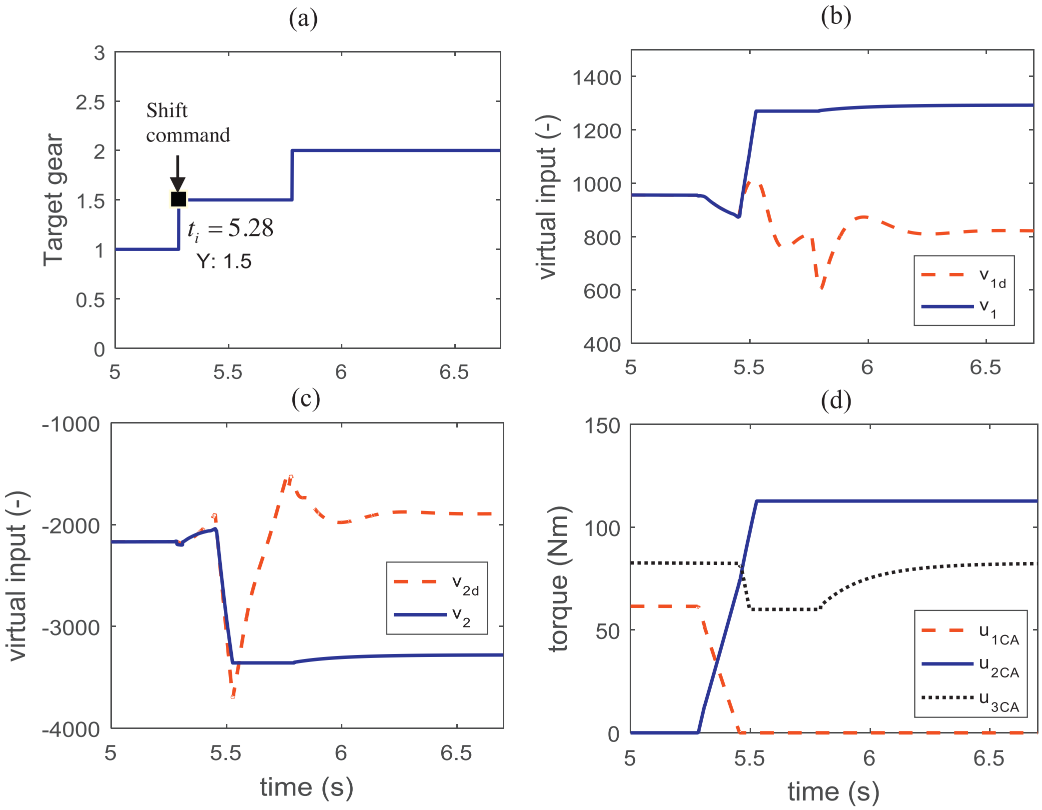

Fig. 7. Upper level control for Case 3 ($W_v = [7\ 0; 0\ 7]$): (a) target gear, (b) virtual input 1, (c) virtual input 2, and (d) resulting allocated torques.

(f)). After the gear shift, further increments of the on-coming clutch force are potentially required in order to guarantee its strong engagement.

Case 2: $W_v = [1\ 0; 0\ 10]$

In Case 2, the weighting factor is tuned in the opposite way to Case 1. The results are presented in Figs. 5 and 6.

As expected, the tracking performance of v_2 is enhanced while that of v_1 is not. The allocated torque trajectory of the on-coming clutch is characterized by its fast increasing torque rate in inertia phase to shorten its synchronization time.

Because the upper level control was tuned to focus more on the shift speed than the shift comfort, the responses of a fast shift with a relatively non-smooth vehicle acceleration are expected. At the beginning of inertia phase, the on-coming clutch force rapidly increased to allow fast increment of the corresponding torque through it (Fig. 6(a) and (b)). Thus, when the engine torque was abruptly reduced by the throttle controller, the torque of the on-coming clutch remained a very high value (>120 Nm) that leads to its faster synchronization with the engine than Case 1. However, the large transmitted torque through the on-coming clutch significantly increased the output torque overshoot (Fig. 6(e)). Then, the output torque tended to decrease as the engine controller reduced the engine torque while the on-coming clutch and engine were being synchronized. As a result, the lock-up time of the on-coming clutch, or the shift time, was much shorter in Case 2 than in Case 1 (Fig. 6(f)), while the ride quality was significantly worse (Fig. 6(h)).

Case 3: $W_v = [7\ 0; 0\ 7]$

In order to further demonstrate the novelty of the proposed control scheme, another simulation was conducted using an equally assigned weighting factor, i.e. $W_v = [7\ 0; 0\ 7]$. The weighting value is determined such that the magnitudes of γW_v are approximately the same for all cases, i.e. $\gamma \|W_v\| = 10^5\sqrt{10^2+1^2} = 10^5\sqrt{1^2+10^2} \approx 10^5\sqrt{7^2+7^2}$.

Due to the equally assigned weighting elements, the tracking performances of v_1 and v_2 were comparable, but neither was perfect (Fig. 7(b) and (c)).

In Fig. 8, the results exhibit moderate performances that are between Cases 1 and 2 in terms of both ride quality and shift speed. Table 2 compares several quantitative performances of the three cases. In the comparison of the shift comfort during a gear shift, the peak values of the vehicle acceleration and jerk as well as the magnitude of torque dip were calculated for each case. The torque dip was evaluated by subtracting the minimum output torque in torque phase ($T_{o,\min\_TP}$) from output torque at the shift initiation time ($T_o(t_i)$). Assuming that the lock-up time (t_f) of the on-coming clutch indicates the end of the shifting, the shift time was evaluated through subtracting t_i from t_f. In addition, as an another criterion, the frictional

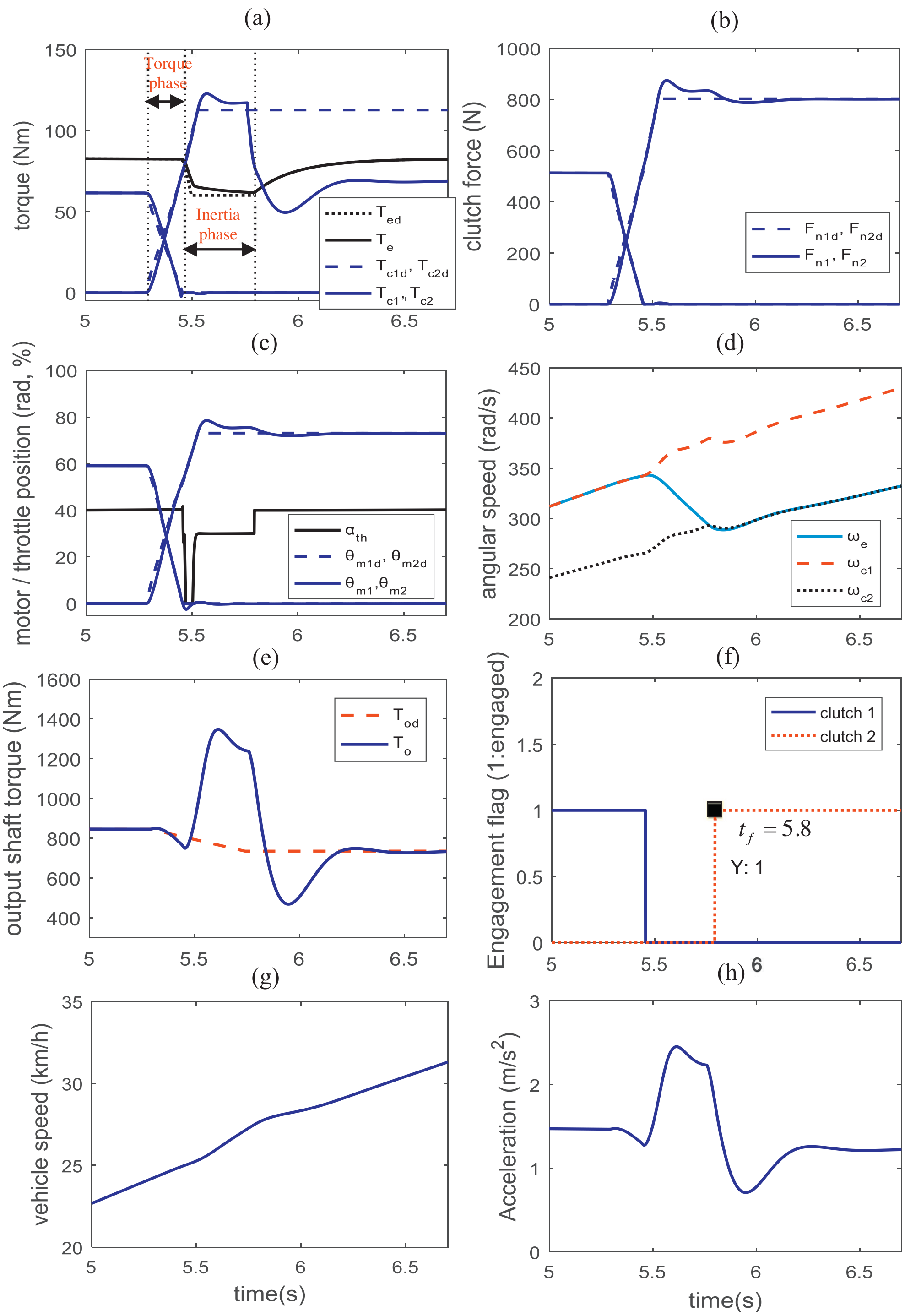

Fig. 8. Lower level control in Case 3 ($W_v = [7\ 0; 0\ 7]$): (a) torque, (b) clutch force, (c) actuator position, (d) speed, (e) output torque, (f) engagement flag, (g) vehicle speed, and (h) vehicle acceleration.

energy (E_d) dissipated in the clutches during the shift was calculated for each case using (30).

$$E_d = \int_{t_i}^{t_f} T_{c1}(\omega_{c1} - \omega_d) + T_{c2}(\omega_d - \omega_{c2})dt \tag{30}$$

As expected from the simulations, Case 1 exhibited the highest performance regarding the peak acceleration and jerk among the three cases, while Case 2 exhibited the shortest shift time. Note that Case 2 also performed the best for the clutch frictional losses. The results of Case 3 where the desired performances were identically weighted had moderate ability for all criteria. It is worth noting that the resulting torque dip values for all cases are exactly the same and small enough to have little effect on the ride quality. That is because the control allocator considered the physical constraint that the off-going clutch is in engaged state during the torque phase, leading to a decrease of the number of active inputs; thus, the solution of u_{CA} was uniquely determined regardless of the weighting factor. Thus, it can be concluded that the shift controller should be tuned focusing mainly on the trade-off between a fast shift and a comfortable shift in inertia phase.

In the simulations, it is observed that the torque transmitted through the on-coming clutch is dominant in determining the magnitude of lock-up overshoot in inertia phase. Also, as the on-coming clutch torque is larger in inertia phase, the duration of the inertia phase is decreased by the same effort of engine throttle control. The shifting performances are governed mainly by the inertia phase control, but appropriate torque phase control is essential to maximize the effectiveness of the inertia phase control. If the torque phase control is performed properly to minimize the shift transient where both clutches are slipping simultaneously, the inertia phase control methods originally aimed at AMTs can be directly used for DCTs.

Consequently, it was demonstrated that the gear shift performances can be adjusted as desired using the proposed control scheme through calibrating one weighting factor, and also that the optimized torque trajectories generated by the control allocator can be used as reference torque values for the integrated controls of the clutches and engine.

5. Conclusion

This paper proposed a novel strategy for the coordinated control of clutches and engine throttle for the gear shift process of a DCT using optimal control allocation. Founded in the idea that a DCT is an over-actuated system with actuator redundancy, the control scheme comprised of upper and lower level parts was developed in order to optimally control the two clutches and engine throttle. This study focuses particularly on the development of a new upper level controller using optimal control allocation. The developed upper level controller generates the desired torque trajectories of the two clutches and engine in terms of the shift requirements with appropriate physical constraints. While the upper level controller assigns the reference torque values for the three actuators in real time, the lower level controller is designed so that it tracks the reference values rapidly considering the actuator dynamics. Using the proposed control scheme, the resulting shift performances can be easily adjusted through tuning only one parameter, and its effectiveness was validated through various simulations where the trade-off between a fast shift and a comfortable shift was noticed. The proposed control structure requires an accurate model of the DCT powertrain including clutch friction information to ensure its high control performance, but there has been a great deal of research concerning the powertrain model development and parameter estimations. This study provides quantitative guidance and insights for how to control the two clutches and engine during the gear shift.

Acknowledgment

This research was supported by the Ministry of Science, ICT and Future Planning (MSIP), Korea, under the Information Technology Research Center (ITRC) (grant no. IITP-2016-H8601-16-1005) supervised by the Institute for Information & Communications Technology Promotion (IITP) and a National Research Foundation of Korea (NRF) grant funded by the Korean government (MSIP) (No. 2010-0028680).

This work was also supported by the BK21+ program through the NRF funded by the Ministry of Education of Korea.

Appendix

1. Active set algorithm

Let u^0 be a feasible starting point satisfying (A2) and (A3).

$$\min_u \|Au - b\| \tag{A1}$$

$$Bu = v \tag{A2}$$

$$Cu \geq U \tag{A3}$$

where $C = \binom{I}{-I}$ and $U = \binom{\underline{u}}{-\bar{u}}$.

Let the working set w contain (a subset of) the active inequality constraints at u^0.

For $i = 0, 1, 2, \ldots$.

Given a suboptimal iterate u^i, find the optimal perturbation p, considering the inequality constraints in the working set as equality constraints and ignoring the remaining inequality constraints. Solve

$$\min_p \|A(u^i + p) - b\|,$$
$$Bp = 0,$$
$$p_i = 0, \ i \in w.$$

If $u^i + p$ is feasible
Set $u^{i+1} = u^i + p$and compute the Lagrange multipliers in (A4).

$$A^T(Au - b) = \begin{pmatrix} B^T & C_0^T \end{pmatrix} \begin{pmatrix} \mu \\ \lambda \end{pmatrix}, \tag{A4}$$

where C_0 is composed of the rows of C corresponding to constraints in the working set.
If all $\lambda \geq 0$
u^{i+1} is the optimal solution to (A1)–(A3).
else
Remove the constraint associated with the most negative λ from the working set.
else
Determine the maximum step length α such that $u^{i+1} = u^i + \alpha p$ is feasible. Add the bounding constraint at u^{i+1} to the working set.

2. Weighted least squares (WLS) control allocation using active set method

(1) Let w and u^0 be the resulting working set and the corresponding optimal point from the previous sampling instant.
(2) Rewrite the cost function in (14) as

$$\|W_u(u - u_r)\|^2 + \gamma\|W_v(Bu - v)\|^2 = \left\| \begin{pmatrix} \gamma^{\frac{1}{2}} W_v B \\ W_u \end{pmatrix} u - \begin{pmatrix} \gamma^{\frac{1}{2}} W_v v \\ W_u u_r \end{pmatrix} \right\|^2.$$

(3) Solve

$$u_{CA} = \arg\min_u \|A'u - b'\|,$$
$$\underline{u} \leq u \leq \bar{u}$$

where

$$A' = \begin{pmatrix} \gamma^{\frac{1}{2}} W_v B \\ W_u \end{pmatrix}, \ b' = \begin{pmatrix} \gamma^{\frac{1}{2}} W_v v \\ W_u u_r \end{pmatrix},$$

using the active set algorithm.

References

[1] Y. Zhang, X. Chen, X. Zhang, W. Tobler, H. Jiang, Dynamic modeling of a dual-clutch automated lay-shaft transmission, in: ASME 2003 International Design Engineering Technical Conferences and Computers and Information in Engineering Conference, 2003, pp. 703–708.
[2] E. Galvagno, M. Velardocchia, A. Vigliani, Dynamic and kinematic model of a dual clutch transmission, Mech. Mach. Theory 46 (2011) 794–805.
[3] Y. Liu, D. Qin, H. Jiang, Y. Zhang, Shift control strategy and experimental validation for dry dual clutch transmissions, Mech. Mach. Theory 75 (2014) 41–53.
[4] K. van Berkel, T. Hofman, A. Serrarens, M. Steinbuch, Fast and smooth clutch engagement control for dual-clutch transmissions, Control Eng. Pract. 22 (2014) 57–68.
[5] S. Bai, R.L. Moses, T. Schanz, and M.J. Gorman, “Development of a new clutch-to-clutch shift control technology,” SAE Technical Paper 0148-7191, 2002.
[6] B.Z. Gao, H. Chen, K. Sanada, Y. Hu, Design of clutch-slip controller for automatic transmission using backstepping, Mechatron. IEEE/ASME Trans. 16 (2011) 498–508.
[7] B. Gao, H. Chen, J. Li, L. Tian, K. Sanada, Observer-based feedback control during torque phase of clutch-to-clutch shift process, Int. J. Veh. Des. 58 (2012) 93–108.
[8] X. Song, Z. Sun, Pressure-based clutch control for automotive transmissions using a sliding-mode controller, Mechatron. IEEE/ASME Trans. 17 (2012) 534–546.
[9] P.D. Walker, N. Zhang, R. Tamba, Control of gear shifts in dual clutch transmission powertrains, Mech. Syst. Signal Process. 25 (2011) 1923–1936.
[10] L. Glielmo and F. Vasca, “Optimal control of dry clutch engagement,” SAE Technical Paper 0148-7191, 2000.
[11] F. Garofalo, L. Glielmo, L. Iannelli, F. Vasca, Smooth engagement for automotive dry clutch, in: Decision and Control, 2001. Proceedings of the 40th IEEE Conference on, 2001, pp. 529–534.
[12] L. Glielmo, L. Iannelli, V. Vacca, F. Vasca, Gearshift control for automated manual transmissions, Mechatron. IEEE/ASME Trans. 11 (2006) 17–26.
[13] F. Winchell and W. Route, “Ratio changing the passenger car automatic transmission,” SAE Technical Paper 0148-7191, 1961.
[14] M. Pettersson, L. Nielsen, Gear shifting by engine control, IEEE Trans. Control Syst. Technol. 8 (2000) 495–507.
[15] D. Kim, H. Peng, S. Bai, J.M. Maguire, Control of integrated powertrain with electronic throttle and automatic transmission, IEEE Trans. Control Syst. Technol. 15 (2007) 474–482.
[16] M. Goetz, M. Levesley, D. Crolla, Dynamics and control of gearshifts on twin-clutch transmissions, Proc. Inst. Mech. Eng. Part D 219 (2005) 951–963.
[17] M. Kulkarni, T. Shim, Y. Zhang, Shift dynamics and control of dual-clutch transmissions, Mech. Mach. Theory 42 (2007) 168–182.
[18] J.J. Oh, S.B. Choi, J. Kim, Driveline modeling and estimation of individual clutch torque during gear shifts for dual clutch transmission, Mechatronics 24 (2014) 449–463.

[19] J.J. Oh, S.B. Choi, Real-time estimation of transmitted torque on each clutch for ground vehicles with dual clutch transmission, Mechatron. IEEE/ASME Trans. 20 (2015) 24–36.
[20] O. Härkegård, Backstepping and Control Allocation with Applications to Flight Control, 2003, Ph.D. dissertation, Linköpings universitet, Linköping, Sweden.
[21] O. HäRkegåRd, S.T. Glad, Resolving actuator redundancy—optimal control vs. control allocation, Automatic 41 (2005) 137–144.
[22] J. Tjonnas, T.A. Johansen, Stabilization of automotive vehicles using active steering and adaptive brake control allocation, IEEE Trans. Control Syst. Technol. 18 (2010) 545–558.
[23] B. Schofield, T. Hagglund, Optimal control allocation in vehicle dynamics control for rollover mitigation, in: 2008 American Control Conference, 2008, pp. 3231–3236.
[24] A. Crowther, N. Zhang, D. Liu, J. Jeyakumaran, Analysis and simulation of clutch engagement judder and stick-slip in automotive powertrain systems, Proc. Inst. Mech. Eng. Part D 218 (2004) 1427–1446.
[25] J. Kim, S.B. Choi, Design and modeling of a clutch actuator system with self-energizing mechanism, Mechatron. IEEE/ASME Trans. 16 (2011) 953–966.
[26] J. Oh, J. Kim, S. Choi, Design of self-energizing clutch actuator for dual clutch transmission, Mechatron. IEEE/ASME Trans. (2015) PP.
[27] T.J. Thor, D.W. Wright, B.J. Pellerito, and C.A. Brunstetter, "Resolving tie-up in a clutch-to-clutch transmission," ed: US Patent Application 7559873 B2, 2009.
[28] L.T. Nitz and R.S. Milunas, "Engine torque management for engine speed flare suppression for clutch-to-clutch-upshifting," ed: US Patent Application 5129286 A, 1992.
[29] Y. Liu, D. Qin, H. Jiang, Y. Zhang, A systematic model for dynamics and control of dual clutch transmissions, J. Mech. Des. 131 (2009) 061012.
[30] J. Kim, K. Cho, S.B. Choi, Gear shift control of dual clutch transmissions with a torque rate limitation trajectory, in: American Control Conference (ACC), 2011, 2011, pp. 3338–3343.
[31] A. Szadkowski and G.J. McNerney, "Clutch engagement simulation: engagement with throttle," SAE Technical Paper 0148-7191, 1992.
[32] M. Hoic, Z. Herold, N. Kranjcevic, J. Deur, V. Ivanovic, Experimental characterization and modeling of dry dual clutch thermal expansion effects, SAE Int. J. Passenger Cars-Mech. Syst. 6 (2013) 775–785.
[33] A. Myklebust, L. Eriksson, Modeling, observability, and estimation of thermal effects and aging on transmitted torque in a heavy duty truck with a dry clutch, IEEE/ASME Trans. Mechatron. 20 (2015) 61–72.
[34] L.P. Russo, B.W. Bequette, State-space versus input/output representations for cascade control of unstable systems, Ind. Eng. Chem. Res. 36 (1997) 2271–2278.
[35] F. Vasca, L. Iannelli, A. Senatore, G. Reale, Torque transmissibility assessment for automotive dry-clutch engagement, Mechatron. IEEE/ASME Trans. 16 (2011) 564–573.